

Next-generation transcatheter aortic valve implantation



Hong-Gook Lim, MD, PhD,^a Saeromi Jeong, MS,^a Gi Beom Kim, MD, PhD,^b Whal Lee, MD, PhD,^c Kuk Hui Son, MD, PhD,^d and Yong Jin Kim, MD, PhD^e

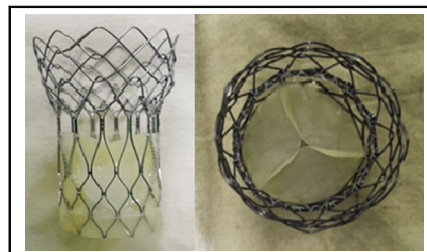
ABSTRACT

Objective: Transcatheter aortic valve implantation (TAVI) procedures are increasing rapidly, but the durability of tissue valve and periprocedural complications are not satisfactory. Immune reaction to the galactose- α -1,3 galactose β -1,4-N-acetylglucosamine (α -Gal) and conventional processing protocols of cardiac xenografts lead to calcification. Next-generation TAVI needs to be made with α -Gal-free xenografts by multiple anticalcification therapies to avoid immune rejection and enhance durability, and three-dimensional (3D) printing technology to improve the procedural safety.

Methods: Porcine pericardia were decellularized and immunologically modified with α -galactosidase. The pericardia were treated by space filler, crosslinked with glutaraldehyde in organic solvent, and detoxified. The sheep-specific nitinol (nickel-titanium memory alloy) wire backbone was made from a 3D-printed model for ovine aortic root. After it passed the fitting test, we manufactured a self-expandable stented valve with the porcine pericardia mounted on the customized nitinol wire-based stent. After in vitro circulation using customized silicone aortic root, we performed TAVI in 9 sheep and obtained hemodynamic, radiological, immunohistopathological, and biochemical results.

Results: The valve functioned well, with excellent stent fitting and good coronary flow under in vitro circulation. Sheep were sequentially scheduled to be humanely killed until 238 days after TAVI. Echocardiography and cardiac catheterization demonstrated good hemodynamic status and function of the aortic valve. The xenografts were well preserved without α -Gal immune reaction or calcification based on the immunological, radiographic, microscopic, and biochemical examinations.

Conclusions: We proved preclinical safety and efficacy for next-generation α -Gal-free TAVI with multiple anticalcification therapies and 3D-printing technology. A future clinical study is warranted based on these promising preclinical results. (JTCVS Open 2020;3:14-24)



Transcatheter aortic valve from α -Gal-free porcine pericardia on customized nitinol stent.


CENTRAL MESSAGE

Next-generation α -Gal-free transcatheter aortic valve implantation with multiple anticalcification therapies and 3D printing technology enhances durability of valve and minimize complications.

PERSPECTIVE

This preclinical study demonstrated that α -Gal-free xenografts by multiple anticalcification therapies were well preserved without immune reaction, and nitinol wire-based stent customized by 3D printing technology enhanced accurate fixation inside aortic root. A future clinical study for next-generation transcatheter aortic valve implantation is warranted based on these promising preclinical results.

See Commentary on page 25.

 Video clip is available online.

From the Departments of ^aThoracic and Cardiovascular Surgery, ^bPediatrics, and ^cRadiology, Seoul National University Hospital, Seoul National University College of Medicine, Seoul; ^dDepartment of Thoracic and Cardiovascular Surgery, Gachon University Gil Medical Center, Gachon University, Incheon; and ^eDepartment of Thoracic and Cardiovascular Surgery, Sejong General Hospital, Bucheon, Korea. This study was supported by TaeWoong Medical Co, Ltd.

Received for publication June 14, 2020; revisions received June 14, 2020; accepted for publication June 17, 2020; available ahead of print July 20, 2020.

Address for reprints: Yong Jin Kim, MD, PhD, Department of Thoracic and Cardiovascular Surgery, Sejong General Hospital, 51-7, Hohyeon-ro 489beon-gil, Bucheon-si, Gyeonggi-do 14755, South Korea (E-mail: yjkim7148@naver.com). 2666-2736

Copyright © 2020 The Authors. Published by Elsevier Inc. on behalf of The American Association for Thoracic Surgery. This is an open access article under the CC BY-NC-ND license (<http://creativecommons.org/licenses/by-nc-nd/4.0/>). <https://doi.org/10.1016/j.jxjon.2020.06.008>

Transcatheter aortic valve implantation (TAVI) has been predominantly used for treatment of symptomatic severe aortic stenosis, and indications for TAVI have been expanded from patients at high risk or with old age toward low-risk or young patients.¹ However, durability, hemodynamics, periprocedural safety, and long-term adverse events associated with TAVI have not been satisfactory.^{2,3} Conventional management strategies are less efficient due to time-dependent and frequent structural valve degeneration of transcatheter heart valves consisting of thrombus formation,

Abbreviations and Acronyms

3D	= 3-dimensional
α -Gal	= galactose- α -1,3 galactose β -1,4-N-acetylglucosamine
α -Gal KO	= α 1,3-galactosyltransferase knockout
BSA	= bovine serum albumin
GA	= glutaraldehyde
TAVI	= transcatheter aortic valve implantation

endothelial hyperplasia, fibrosis, tissue remodeling, and calcification.³⁻⁶

Immune reaction to the galactose- α -1,3 galactose β -1,4-N-acetylglucosamine (α -Gal) of cardiac xenografts leads to calcification.^{7,8} Conventional glutaraldehyde (GA) crosslinking and anticalcification protocols of cardiac xenografts don't avoid bioprosthetic valve failure caused by immune rejection^{9,10} and deleterious effects of tissue phospholipids, conformational changes in collagen, and free aldehyde groups.¹¹ Therefore, future directions for TAVI should include the avoidance of immune rejection by α -Gal-free xenografts^{7,8} and enhanced durability by multiple anticalcification therapies and novel tissue treatments.¹¹⁻¹³

Current commercialized TAVI also causes serious complications, which include paravalvular leakage, aortic regurgitation, aortic stenosis, complete atrioventricular block requiring permanent pacemaker implantation, stent migration, coronary obstruction, and myocardial infarction.^{2,3} The complication of new-onset atrioventricular and intraventricular conduction block is most common,^{1,14} and the complication of prosthesis dislocation is the most important.^{1,15} Alternative strategies are needed to avoid such complications.^{1-3,14,15}

To solve current issues related to periprocedural safety, a stented valve for TAVI should be customized by 3-dimensional (3D) printing technology.¹⁶ In this study, we proved the first preclinical safety and efficacy for next-generation TAVI.

MATERIALS AND METHODS**Decellularization**

Porcine pericardia were washed in 0.9% normal saline, and then 0.1% peracetic acid with 4% ethanol in distilled water for 1 hour and then washed for 2 hours with distilled water. These tissues were initially treated with hypotonic buffered solution containing 0.25% sodium dodecyl sulfate for 24 hours at 4°C and washed with distilled water for 1 hour. Later, they were treated with hypotonic solution containing 0.5% Triton X-100 for 24 hours at 4°C and washed with distilled water for 12 hours at 4°C. These tissues were then treated with isotonic solution for 24 hours at 4°C and were finally treated with hypertonic buffered solution (II) for 6 hours at 4°C and washed with phosphate-buffered saline (PBS) for 1 hour at 4°C.

Construction and Preparation of α 1,3 Galactosidase From *Bacteroides thetaiotaomicron*

The gene for α -galactosidase from *B thetaiotaomicron* (designated BtGal110B) was amplified from the corresponding genomic DNAs by polymerase chain reaction and was introduced into the pET28a vector for expression of the His₆-tagged proteins using appropriate restriction sites for protein expression in *Escherichia coli* Rosetta2 (DE3; Novagen, Madison, Wis). *E coli* was grown in Luria-Bertani media supplemented with 34 μ g/mL chloramphenicol and 30 μ g/mL kanamycin induced at an A_{600 nm} ~0.6 with 1 mM isopropyl-1-thio- β -D-galactopyranoside. The harvested cell pellet was lysed in a lysis buffer (50 mM NaH₂PO₄, 300 mM NaCl, and 10 mM imidazole) using an Ultrasonicator (Misonix Inc, Farmingdale, NY). The crude lysates were centrifuged for 20 minutes at 13,000 rpm, at 4°C and the expressed protein was purified using a Nickel-NTA agarose column (QIAGEN, Valencia, Calif) according to the manufacturer's instruction.

Immunologic Modification by Inactivating Xenoantigens (α -Gal)

The porcine pericardia were treated with 0.1 units/mL α -galactosidase for 24 hours at 4°C.

Space-Filler Treatment

The porcine pericardia were treated with 30% polyethylene glycol (1000 MW) in 0.01 M PBS (pH 7.4) for 1 day at 4°C.

GA Fixation in Organic Solvent

The porcine pericardia were initially fixed with 0.5% GA for 3 days at room temperature, additionally fixed with 0.25% GA in organic solvent of 75% ethanol + 5% octanol for 2 days at room temperature, and finally fixed in 0.25% GA for 7 days at room temperature.

Detoxification

After completion of fixation, the porcine pericardia were treated with 0.2M glycine solution (PBS, pH 7.4) at room temperature for 24 hours.

Manufacture of Sheep-Specific Transcatheter Aortic Valve

Sheep underwent electrocardiographic-gated cardiac computed tomography studies. After converting the Digital Imaging and Communications in Medicine images for ovine aortic root into 3D image using Mimics Base version 16 (Materialize, Leuven, Belgium), the segmented 3D image was stored as a stereolithography file (Figure 1). The file was then sent to 3D printer (uPrint; Stratasys Ltd, Eden Prairie, Minn) and 3D model of the aortic root was printed (Figure 2). For the fitting test and in vitro mock circulation, a hollow elastic model with both coronary arteries was made by painting liquid silicone evenly on the surface of 3D-printed model (Figure 2). The customized jig was made from 3D-printed model for ovine aortic root, and sheep-specific nitinol (nickel-titanium memory alloy) wire backbone was made from the jig. The nitinol stent was inserted inside customized silicone aortic root, and fitting test of the stent was performed. After passing the fitting test, α -Gal-free porcine pericardia treated by our anticalcification protocols were mounted on the customized self-expandable nitinol wire-based stent (Figure 3). The valve design for the key dimensions of the prostheses was customized according to the ovine aortic root, and average total axial length was 45 mm, average target implant diameter was 24 mm, average outflow flare diameter was 26 mm, and average length of the sheet height was 19 mm (Figure 3).

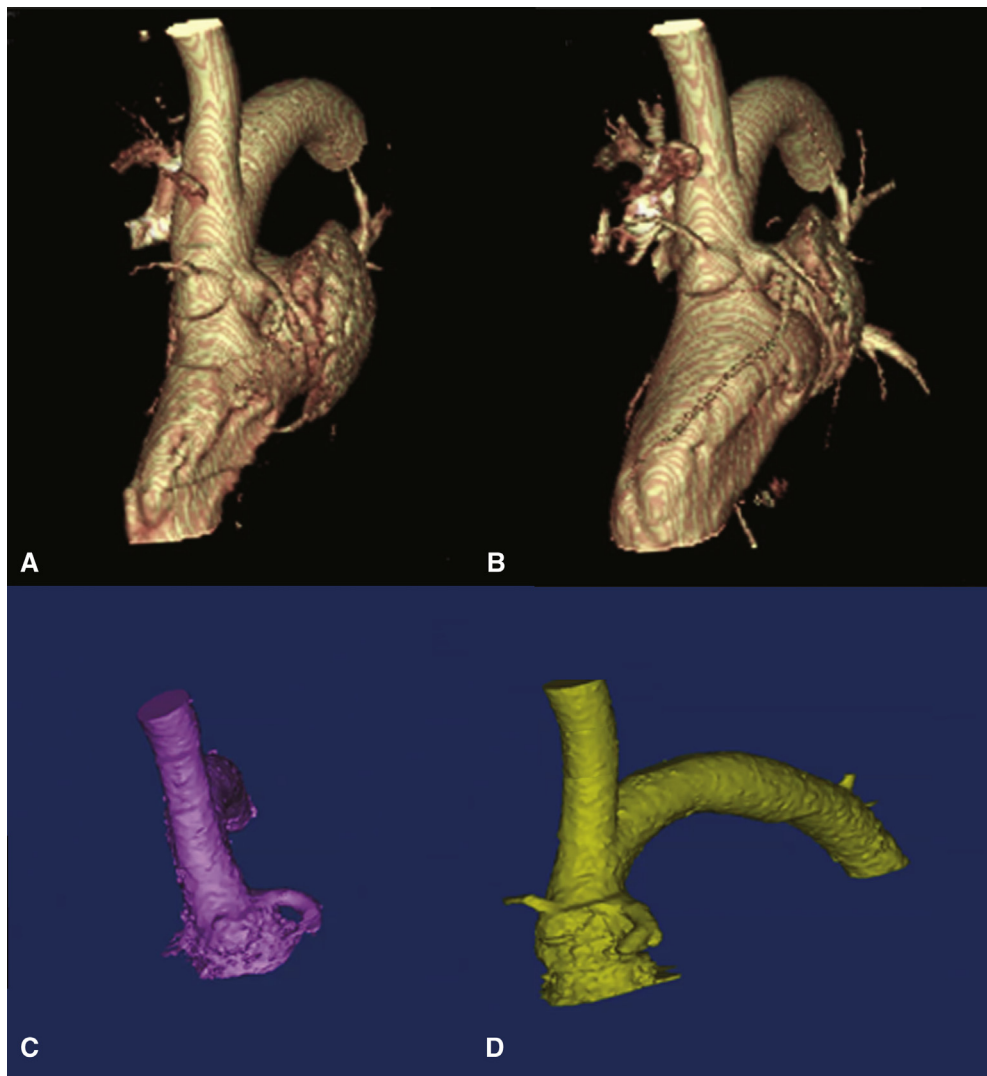


FIGURE 1. Three-dimensional (3D) computed tomography images (A-B) and segmented 3D image stored as a stereolithography file (C-D) for ovine aortic root.

In Vitro Mock Circulation

We developed a specially designed mock circulation model¹⁷ to evaluate stent fitting, valve motion, and coronary patency of the stented valve in vitro. The stented valve was inserted inside customized silicone aortic root, which was connected to our mock circulation circuit and placed under in vitro circulation. The circulation solutions contained normal saline (0.9% NaCl) and 0.1% GA. A pulsatile pressure of 120/80 mm Hg was repetitively provided to the stented valve at a constant interval of 60 rpm in one direction to reproduce in vivo circulation. Both coronary arteries were connected into 3-way stopcocks with extension tubing, and coronary flow returned into in vitro mock circulation (Figures 2 and 4).

Preclinical Study

This study was approved by the Institutional Animal Care and Use Committee of the Clinical Research Institute, Seoul National University Hospital. This facility is accredited by the Association for the Assessment and Accreditation of Laboratory Animal Care

International. Sheep aged approximately 24 months (Daegwanryung, Kangwon-do, Republic of Korea) were prepared, and the weight range was 41~55 kg. Cefazolin was administered intravenously at 20 mg/kg. The sheep were injected intramuscularly with 5 mg/kg Zoletil and 0.25 mg/kg Rompun, as preanesthetics. The sheep were endotracheally intubated and anesthetized with 1.3~2.0% enflurane in O₂ and instrumented for hemodynamic monitoring. The sheep were placed in the left lateral decubitus position under general anesthesia. The right cervical area was cut to expose the common carotid artery. After insertion of a 5-Fr sheath in the carotid artery, routine hemodynamic study and angiography were performed. The self-expandable valved stents of 23~26 mm diameter were loaded into 18~22 Fr delivery system and were implanted using a retrograde transarterial approach. Angiography, fluoroscopy, and echocardiography were used to guide the deployment into a good position inside the aortic root by controlling the catheter handle meticulously. After the self-expandable valved stent implantation, transthoracic echocardiography and cardiac catheterization were performed to evaluate hemodynamic changes. The care after TAVI consists of continuous routine monitoring with the

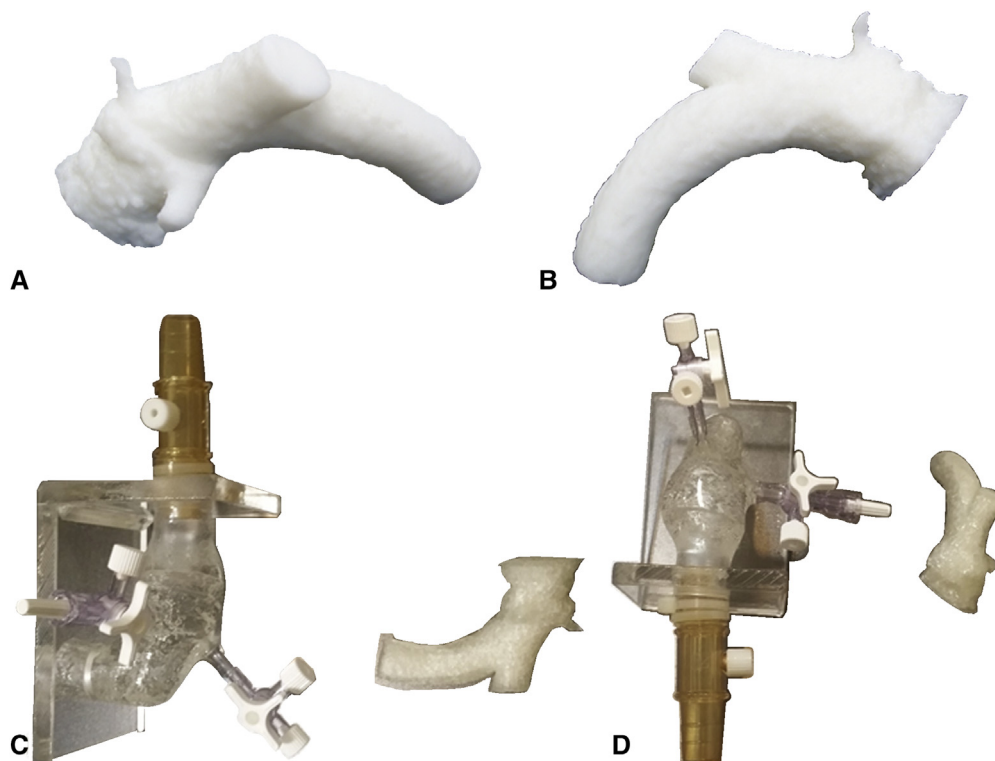


FIGURE 2. Three-dimensional (3D)-printed models (A-B) for ovine aortic root and hollow elastic model with both coronary arteries (C-D) made by painting liquid silicone evenly on the surface of 3D model.

electrocardiogram, oxygen saturation, blood pressure and central venous pressure, and administration of drugs and fluid. The sheep was transferred to the cage after vital signs were stabilized. The clinical courses such as dietary intake, systemic conditions, thromboembolic events, and heart failure were closely observed. Cefazolin (20 mg/kg, once/day for 3 days) was administered intravenously.

Immunoassay

Blood samples were taken from the sheep. An enzyme-linked immunosorbent assay was used to measure the specific serum antibody concentrations (IgM and IgG) against α -Gal in the sheep. Microtiter plates were coated with 100 μ L per well of bovine serum albumin (BSA) conjugating synthesized α -Gal (α -Gal-BSA; Dextra Laboratories, Reading, United Kingdom) in PBS (pH 7.4) (at 1 μ g/mL for the IgM and IgG isotypes) and incubated at 37°C for 1 hours. Then, the plates were washed with PBS containing 0.05% (v/v) Tween 20. Sheep sera (100 μ L per well) were added to the α -Gal-BSA-immobilized wells in BSA-Tween 20 (PBS, pH 7.4, 3% BSA, 0.01% Tween 20), and the plates were incubated for 1 hour at 37°C. Horseradish peroxidase-conjugated rabbit anti-sheep IgM and IgG (AbD SeroTec, Oxford, United Kingdom) were used as the secondary antibody (1:10,000) at the IgM and IgG dilution in BSA-Tween 20. A color reaction was developed with 3,3',5,5'-tetramethylbenzidine solution (BD Biosciences, San Diego, Calif). Absorbance was measured at 450 nm in an enzyme-linked immunosorbent assay reader.

Radiologic Confirmation by Quantifying Calcification

After the sheep were humanely killed, harvested stent valves were cut longitudinally for a thorough visual inspection and tested for radiologic confirmation with simple radiographs.

Calcium Analysis

Harvested tissue samples were washed in normal saline, dried at 70°C for 24 hours, and weighed. The samples were then hydrolyzed with 5.0N HCl solution. The calcium content of the hydrolysate was measured colorimetrically using the o-cresolphthalein complex-one method and an automatic chemistry analyzer (Hitachi 7070, Tokyo, Japan). Calcium content was expressed as μ g/mg dry weight.

Microscopic Examination

Representative tissue samples were examined under light microscopy. The tissue samples were fixed in 10% formalin, embedded in paraffin, and 2- to 4- μ m-thick sections were stained with hematoxylin-eosin, Masson's trichrome, and the von Kossa method.

Immunohistochemistry Staining

Representative tissue samples were stained for sheep macrophages and T cells. The primary antibodies used were anti-sheep F4/80 antigen (eBioscience, San Diego, Calif) at 1:3000 dilution (marker for sheep macrophages) or anti-sheep CD4 (eBioscience) at 1:1000 dilution (marker for sheep T-cells). The secondary antibody used was horseradish peroxidase-conjugated rabbit anti-sheep IgG (AbD SeroTec, Oxford, United Kingdom) at 1:500 dilution. Diaminobenzidine was used as a chromogen and hematoxylin was used for counterstaining.

Statistical Analysis

Statistical analyses were performed with the SPSS software package (version 25.0; IBM Corp, Armonk, NY). Data were expressed as mean \pm standard deviation. The change in the antibody titer against α -Gal was compared according to the duration after TAVI using repeated-measures analysis of variance (Video 1).

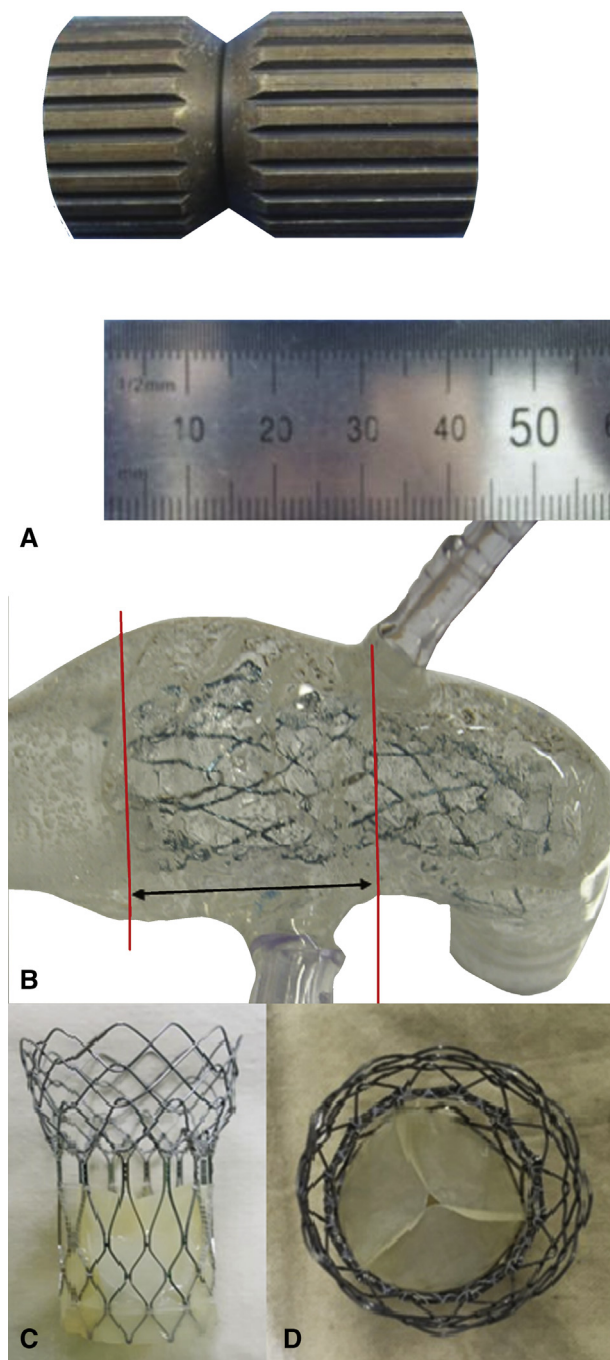


FIGURE 3. Customized jig made from a 3-dimensional–printed model for ovine aortic root (A), fitting test of sheep-specific nitinol (nickel–titanium memory alloy) wire back bone made from the jig inside the customized silicone aortic root (B), and side view (C) and top view (D) of prototype for self-expandable transcatheter aortic valve made from α -Gal–free porcine pericardium mounted on the customized nitinol wire–based stent.

RESULTS

In Vitro Mock Circulation

During the in vitro mock circulation, we confirmed excellent fitting of the stent inside the customized

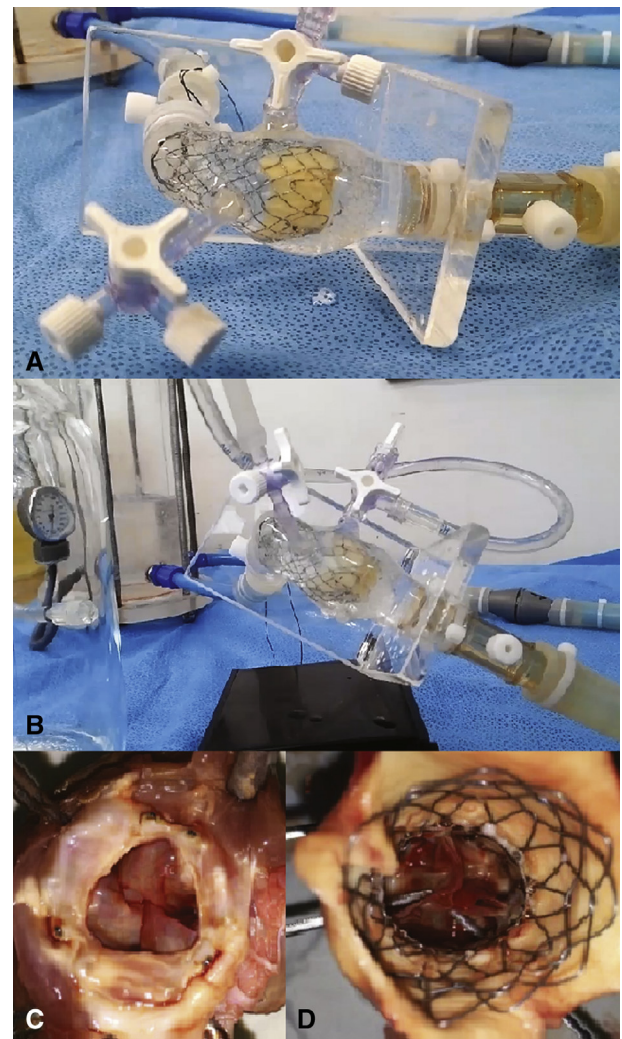


FIGURE 4. Photograph (A–B) of in vitro mock circulation. A pulsatile pressure of 120/80 mm Hg was repetitively provided to the transcatheter aortic valve at a constant interval of 60 rpm in one direction to reproduce in vivo circulation,¹² and good valve motion with excellent fitting of valved stent inside customized silicone aortic root was identified. Both coronary arteries were connected into 3-way stopcocks with extension tubing, and good coronary flow was identified to return into in vitro mock circulation (B). Bottom view (C) and top view (D) of gross findings 196 days after transcatheter aortic valve implantation. All aortic valve leaflets were well mobile without degeneration and calcification (C–D), stent was well endothelialized (C), and both coronary arteries (see 2 forceps inserted into both coronary arteries) were patent above aortic valve (D).

silicone aortic root and good motion of stented valve. Complete alignment of the stent without paravalvular leakage was confirmed within the aortic root, and risks for incomplete deployment within the aortic root were completely avoided under systemic pressure. Both coronary flow was well maintained without obstruction (Figure 4).



VIDEO 1. Development of next generation α -Gal-free transcatheter aortic valve implantation with multiple anticalcification therapies and 3D printing technology. Video available at: [https://www.jtcvs.org/article/S2666-2736\(20\)30057-7/fulltext](https://www.jtcvs.org/article/S2666-2736(20)30057-7/fulltext).

Hemodynamic Study and Gross Findings

After TAVI, 9 sheep were sequentially scheduled to be humanely killed to compare the safety and efficacy of ≤ 1 month of survival ($n = 5$) with ≥ 5 months of survival ($n = 4$). The evaluation of echocardiography and cardiac catheterization demonstrated clinically better outcomes with respect to the control¹⁸⁻²⁰ without stent migration in the same way as in vitro mock circulation for 8 months after TAVI (Table 1). There was no evidence of subclinical thrombosis. None of the explanted aortic valve leaflets showed calcium deposits or plaque and all the explanted aortic valve leaflets remained mobile on gross inspection. Stents were well endothelialized, and both coronary arteries were patent above aortic valve (Figure 4).

Immunological Assay for α -Gal Antibody

The α -Gal IgM antibody titers measured in serum collected before, just after, 1 day~1 month after, and 5~8 months after TAVI were 0.2298 ± 0.0226 , $0.2194 \pm$

0.0181 , 0.2221 ± 0.0079 , and 0.2131 ± 0.0173 , respectively. The α -Gal IgG antibody titers measured during the same schedule were 0.2208 ± 0.0157 , 0.2080 ± 0.0120 , 0.2098 ± 0.0042 , and 0.2174 ± 0.0126 , respectively. No differences in the α -Gal IgM and IgG antibody titer were observed according to the duration after TAVI ($P > .05$).

Specimen Radiography and Analysis of Calcium and Inorganic Phosphorus

Specimen radiography taken from explanted aortic valves demonstrated no calcification for 8 months after TAVI (Figure 5). The calcium and inorganic phosphorus concentrations of the explanted aortic valve leaflets remained very low with $1.59 \pm 0.03 \mu\text{g}/\text{mg}$ and $1.58 \pm 0.05 \mu\text{g}/\text{mg}$ at 2 days after TAVI, and $0.60 \pm 0.01 \mu\text{g}/\text{mg}$ and $0.59 \pm 0.02 \mu\text{g}/\text{mg}$ at 8 months after TAVI.

Microscopic Examination of Explanted Aortic Valve Leaflets After TAVI

For 8 months after TAVI, the collagen fibers appeared well preserved with a normally banded structure, and no specific matrix derangement was noticeable on the hematoxylin-eosin-stained specimens. No cellular nuclei were observed because of complete decellularization. The aortic valve leaflets on Masson’s trichrome stained specimens had a compact array of collagen fibers with preserved structural integrity. The aortic valve leaflets on von Kossa-stained specimens showed no evidence of calcification (Figure 6).

Immunohistochemistry Staining of Explanted Aortic Valve Leaflets After TAVI

In the porcine pericardial tissues implanted into the aortic root of sheep, F4/80 staining revealed no or rare macrophages, and CD4 staining revealed no or rare T cells for 8 months after TAVI (Figures 7 and 8 and Video 1).

DISCUSSION

Currently, TAVI procedures are increasing rapidly, but the durability for tissue valves are not satisfactory, and the

TABLE 1. Timeline of control groups ($n = 28$) compared with this study ($n = 9$)

Group	Position for xenograft implantation	Number according to experiment duration		
		≤ 1 M	1-5 M	≥ 5 M
Study	Aortic position	5*		4†
Control	Aortic position ¹⁸	2‡	3§	3
	Pulmonary position ^{19,20}	6¶	1#	13**
	Total	8	4	16

In the control groups, †† graft failure; ‡¶ was not clearly identified until 1 month after implantation, but graft failure||** was clearly confirmed from 5 months after implantation.¹⁸⁻²⁰ In the study group, †† all grafts*† remained the same as preoperative status without graft failure even after 5 months after implantation. *At 1, 2, 18, 23, and 29 days after xenograft implantation in aortic position (this study). †At 149, 182, 196, and 238 days after xenograft implantation in aortic position (this study). ‡At 5 and 31 days after xenograft implantation in aortic position.¹⁸ §At 40, 40, and 107 days after xenograft implantation in aortic position.¹⁸ ¶At 363, 411, and 636 days after xenograft implantation in aortic position.¹⁸ ¶At 2, 3, 3, 7, 17, and 20 days after xenograft implantation in pulmonary position.^{19,20} #At 102 days after xenograft implantation in pulmonary position.²⁰ **At 147, 195, 224, 264, 340, 361, 362, 471, 497, 573, 591, 598, and 599 days after xenograft implantation in pulmonary position.^{19,20} ††Control groups underwent implantation of porcine xenograft without α -Gal removal and multiple anticalcification therapies. †††Study group underwent implantation of α -Gal-free porcine xenograft treated by multiple anticalcification therapies.

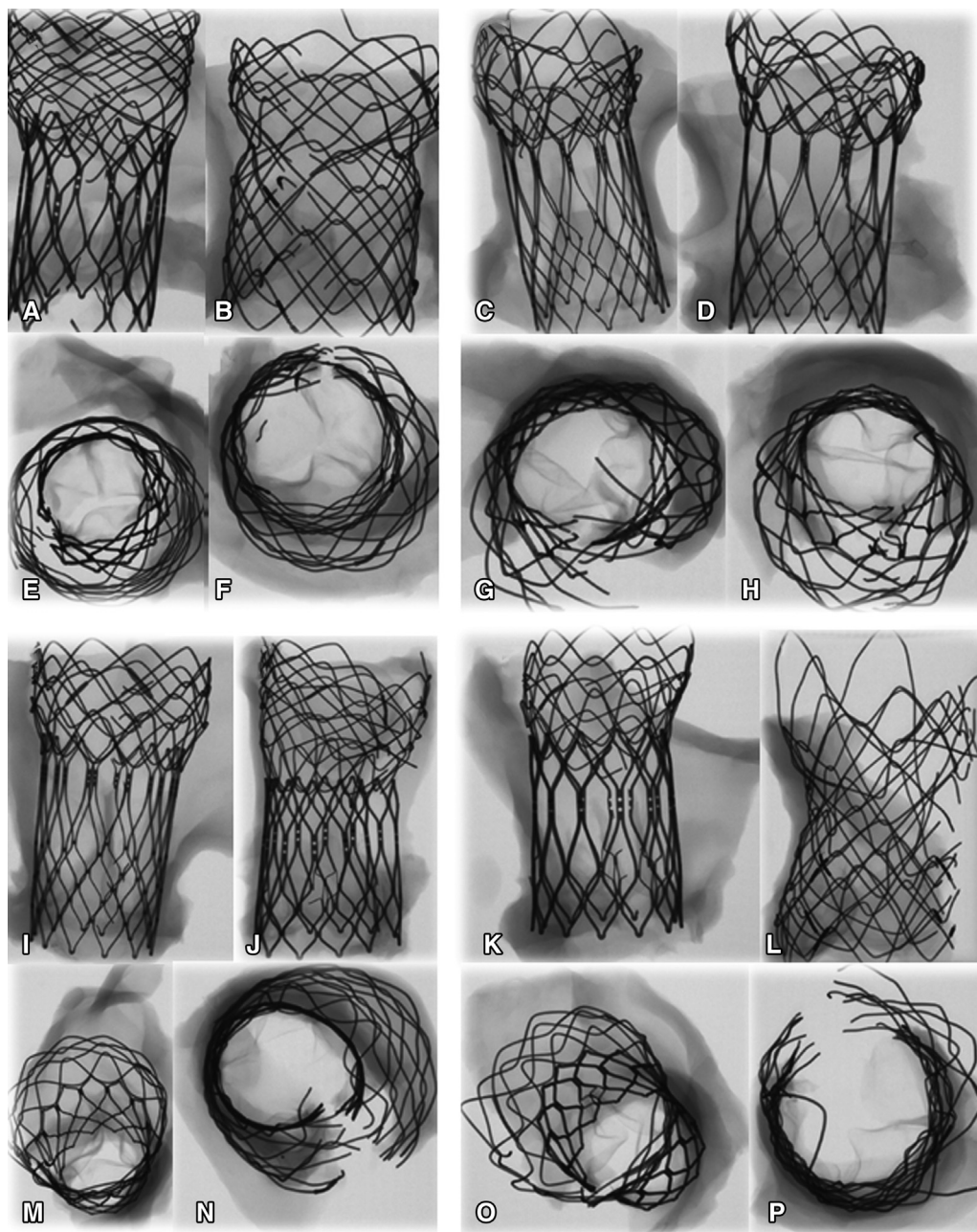


FIGURE 5. Specimen radiographic findings taken from explanted aortic valve after TAVI. *Side view:* 2 (A), 8 (B), 23 (C), 29 (D), 149 (I), 182 (J), 196 (K), and 238 (L) days after TAVI. *Top view:* 2 (E), 8 (F), 23 (G), 29 (H), 149 (M), 182 (N), 196 (O), and 238 (P) days after TAVI. TAVI, Transcatheter aortic valve implantation.

complications such as paravalvular leakage, aortic regurgitation, aortic stenosis, complete atrioventricular block requiring permanent pacemaker implantation, stent migration, coronary obstruction, and myocardial infarction are still challenges to be solved.¹⁻³ In this study, we performed the first in vivo large animal study under aortic position for this α -Gal-free substitute with multiple anticalcification therapies and succeeded in proving the preclinical safety and efficacy for next-generation TAVI. This preclinical

study showed that the function of aortic valves was well maintained without subclinical thrombosis after TAVI with this biocompatible substitute, and the xenografts were well preserved without calcification based on the radiographic, microscopic and biochemical examinations.

In contrast, control experiments of the fresh porcine xenografts¹⁸ implanted to the aortic position of goat resulted in severe calcification, fibrosis, and tissue degeneration. Additional treatment with decellularization also only reduced

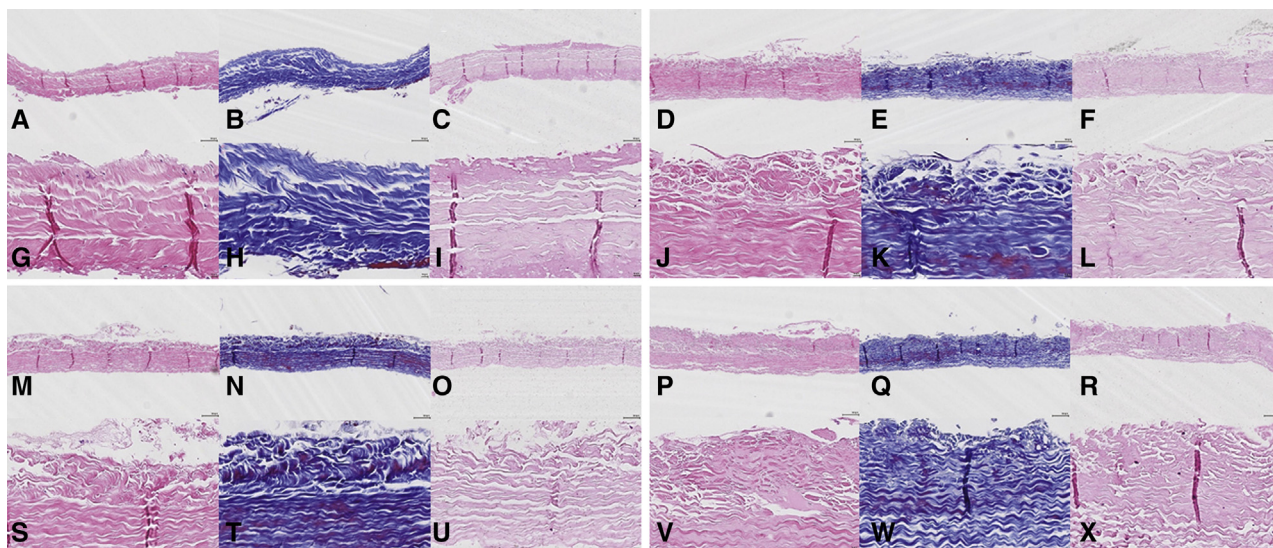


FIGURE 6. Microscopic findings taken from explanted aortic valve leaflet 2 (A, B, C, G, H, I), 29 (D, E, F, J, K, L), 182 (M, N, O, S, T, U), and 196 (P, Q, R, V, W, X) days after TAVI. Hematoxylin–eosin staining (A, D, G, J, M, P, S, V), Masson’s trichrome staining (B, E, H, K, N, Q, T, W), von Kossa staining (C, F, I, L, O, R, U, X), ×100 (A-F, M-R), and ×400 (G-L, S-X). Staining showed well-preserved collagen fibers with normally banded structure, no specific matrix derangement, compact array of collagen fibers with preserved structural integrity, and no calcification for 8 months after TAVI.

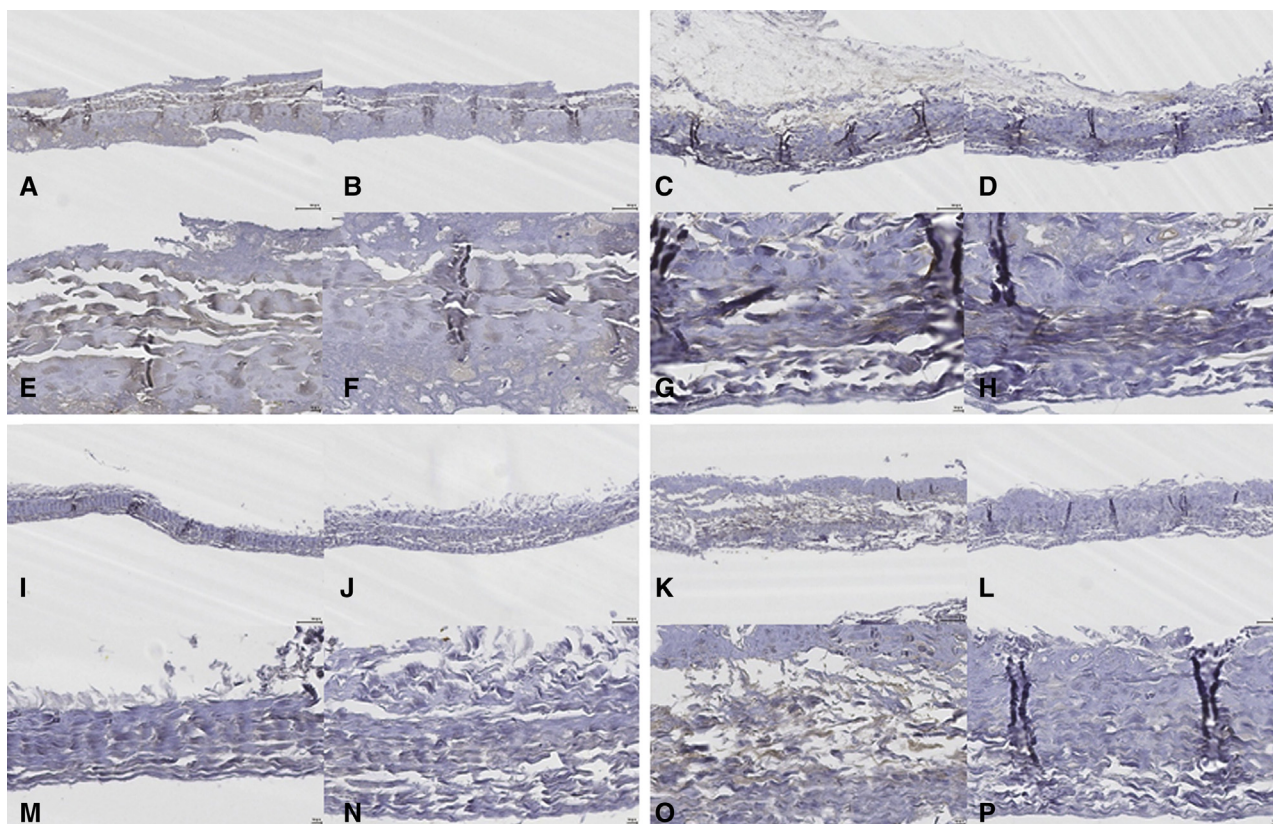


FIGURE 7. Immunohistochemistry stainings taken from explanted aortic valve leaflet 2 (A, B, E, F), 29 (C, D, G, H), 182 (I, J, M, N), and 196 (K, L, O, P) days after TAVI. F4/80 (macrophage) staining (A, C, E, G, I, K, M, O), CD4 (T-cell) staining (B, D, F, H, J, L, N, P), ×100 (A~D, I~L), and ×400 (E~H, M~P). Staining revealed no or rare immune cells for 8 months after TAVI.

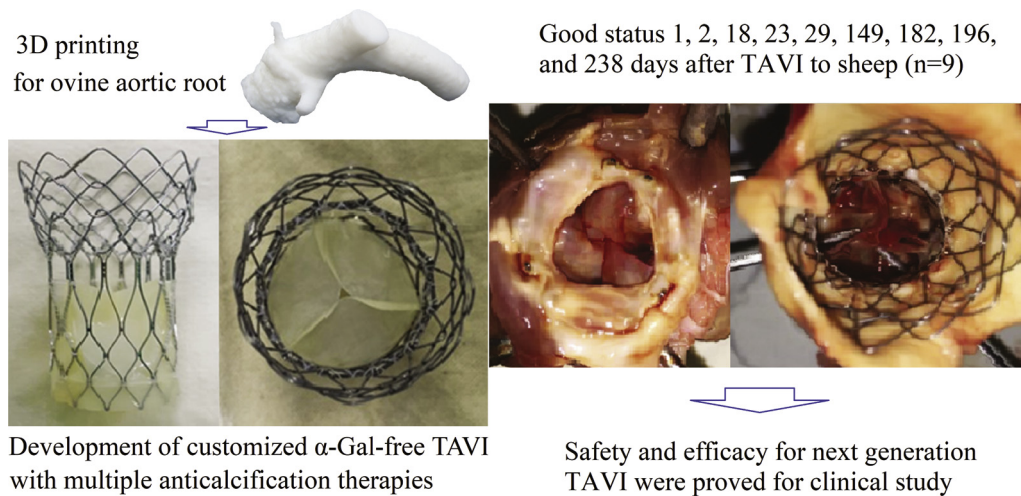


FIGURE 8. Development of next generation α -Gal-free TAVI with multiple anticalcification therapies and 3D printing technology. *3D*, 3-dimensional; *TAVI*, transcatheter aortic valve implantation; α -Gal, galactose- α -1,3 galactose β -1,4-N-acetylglucosamine.

immune reaction to change pathologic findings from neutrophil to lymphocyte infiltration but did not improve long-term durability at all. To improve durability of xenograft, we applied the multistep anticalcification protocols and the synergy mechanisms are as follows: (1) cross-linkage of xenograft tissue with GA obtains stabilization of collagen and suppresses host immunologic reactivity¹¹; (2) detoxification with amino acids neutralizes the residual free aldehyde groups of GA, forming a Schiff base¹¹; (3) organic solvent removes phospholipids and is preferentially bound to hydrophobic residues within collagen and elastin¹¹; and (4) decellularization suppresses residual antigenicity.¹¹ The *in vivo* experiments for small animals proved that our anticalcification protocols of xenograft tissue were effective.¹¹ In pulmonary position, the large-animal long-term circulatory model also proved the safety and efficacy for optimal GA crosslinkings of porcine¹⁹ and bovine²¹ xenograft tissue with our anticalcification treatments compared with those without treatments.^{19,20}

The animal immune response may play an important role in structural damage of the currently commercially available bioprosthetic valves.^{7,9,10} We demonstrated that removing α -Gals from the surface of the xenogenic tissue valves can improve the durability of the xenogenic tissue valves in the experiments for α -Gal KO mice to mimic the human immunologic environment.⁸ In pulmonary position, the large-animal long-term circulatory model also demonstrated the safety and efficacy for our anticalcification protocols including immunologic modification²² compared with control groups.^{19,20}

Space filler prevents calcification of GA-pretreated cardiac xenograft by filling the interstitial void spaces with a macromolecular substance.¹² *In vivo* small animal experiments confirmed the synergistic anti-calcification effect of

space filler for xenograft tissue,¹² and the experiments for humanized (α -Gal KO) mice finally proved that our novel combined anti-calcification protocols including space filler and immunologic modification for xenograft tissue were the most effective.¹³ The large-animal long-term circulatory model demonstrated the preclinical safety and efficacy in pulmonary²³ and mitral¹⁷ position for our novel combined anticalcification protocols including space filler and immunologic modification compared with control groups.¹⁸⁻²⁰

The clinical study demonstrated the safety and efficacy in pulmonary position for our novel combined anticalcification protocols including space filler and immunologic modification.^{24,25} The α -Gal-free bioprosthetic valves were successfully commercialized for the first time in the world, and have been implanted to the pulmonary position of the patients. Currently, clinical trials (The PULSTA Transcatheter Pulmonary Valve Pre-Approval Study, [ClinicalTrials.gov](https://clinicaltrials.gov) Identifier: NCT03983512) for our α -Gal-free bioprosthetic valves to the pulmonary position are also in progress for 5 European countries (Germany, Italy, Netherlands, Spain, Turkey; <https://clinicaltrials.gov/ct2/show/NCT03983512>). In the next step, this preclinical study demonstrated that our α -Gal-free bioprosthetic valves to the aortic position were safe and effective. Specific details are described in the results section.

Humans lack animal antigens (α -Gal), which causes significant animal immune rejection following implantation of porcine or bovine bioprosthetic heart valve. To avoid immune rejection and dramatically improve the durability for bioprosthetic valves, it is necessary to use xenografts from primates or α -Gal KO pigs, which are immunologically similar to humans. However, this commercialization is impossible due to lack of economic feasibility and difficulty of mass production. Instead, we

used enzymatic removal methods with α -galactosidase for cardiac xenografts and confirmed that α -galactosidase effectively removed animal antigens from cardiac xenografts.⁷ We chose the *Bacteroides thetaiotaomicron*-derived recombinant α -galactosidase expressed in *E coli*, which is effective with small amount under physiological conditions, and advantageous in cost effectiveness.⁷ The in vivo study using humanized mice also demonstrated that the enzymatic removal methods with α -galactosidase made cardiac xenografts have excellent anticalcification effects as primate.^{13,26} Sheep was used as preclinical model for porcine xenograft implantation instead of pig. The animal immune response exists between heterogeneous species because the differences in the fine specificity of natural anti-Gal in various species may cause the multiple B-cell clones to produce anti-Gal antibodies that have specificities that differ slightly from each other and thus recognize various “facets” of the α -Gal epitope in its 3D form.¹¹

In the next step, the in vivo study using humanized mice demonstrated that the treatment of α -galactosidase made porcine xenografts more durable than bovine xenografts.²⁷ The clinical study also reported that porcine xenografts were more durable than bovine xenografts, although animal antigens still exist in currently commercialized valves.^{28,29} Therefore, we chose porcine xenografts for the α -Gal-free bioprosthetic valves instead of bovine xenografts and demonstrate the preclinical safety and efficacy for the α -Gal-free porcine xenografts after TAVI in this study. The α -Gal-free porcine xenografts were well preserved without α -Gal immune reaction based on the immunologic examinations.

Self-expandable stents are safer than balloon-expandable stents because the procedures are simple without balloon dilation and the risks of wire-based-stent fracture are low. To improve the completeness of the manufacturing process for the self-expandable nitinol wire backbone, 3D printing mock up for ovine aortic root was used for in vitro mock circulation as well as manufacture of the customized jig and fitting test before the preclinical in vivo study. In this study, the excellent flexibility of our knitted self-expandable nitinol wire-based stent customized by 3D printing technology enhanced tight and accurate fixation inside the aortic root after TAVI, which reduced complications including structural valve deterioration, subclinical thrombosis, paravalvular leakage, complete atrioventricular block requiring permanent pacemaker implantation, stent migration, coronary obstruction, and myocardial infarction even under systemic pressure. The manufacture of a customized jig, fitting test, and in vitro mock circulation using our 3D-printed model further minimized complications after TAVI. The detailed planning and presimulation concerning the individual anatomy and characteristics of the aortic root are essential, given the wide variety of pathologies. Presimulation

with in vitro mock circulation using 3D printing must be performed like this study to correct possible problems and increase the completeness and accuracy of real clinical application.¹⁶

The 3D-printed model should reflect real anatomical and functional variations of the aortic root. However, the current study presents several limitations with respect to its ability to mimic the real aorta. The mechanical properties of our silicone model, such as the tensile strength, yield strength, and elastic modulus, are different from human diseased thoracic aortas. The real thickness, stiffness, compliance, and distensibility of aortic and leaflet wall are also not accurately represented. The silicone model doesn't have real elasticity, which altered its diameter during systole and diastole, and the rigidity and flexibility don't mimic actual thickening and calcification. In the near future, the 3D printers can combine a rigid and a flexible photopolymer, and produce multi-material photopolymer for printing a real model for calcified aortic root.^{16,30} The patient-specific model should more closely resemble those of the human diseased thoracic aorta than the silicone model. This preliminary study is also limited by finite element analysis simulation for proper mechanics and small sample size and early results for TAVI. Much more data are needed to fully evaluate the new device.

CONCLUSIONS

We developed the α -Gal-free tissue valve for TAVI with the simultaneous use of multiple anticalcification therapies such as decellularization, immunologic modification with α -galactosidase, space filler, organic solvent, and detoxification. We proved preclinical safety and efficacy for the next-generation α -Gal-free TAVI with novel tissue treatments and 3D printing technology. Future investigations should be directed toward α -Gal-free substitutes such as our tissue valve for TAVI, and future clinical study for next-generation TAVI is warranted based on our preclinical results using in vitro mock circulation and large-animal in vivo systemic circulatory models.

Conflict of Interest Statement

The authors reported no conflicts of interest.

The *Journal* policy requires editors and reviewers to disclose conflicts of interest and to decline handling or reviewing manuscripts for which they may have a conflict of interest. The editors and reviewers of this article have no conflicts of interest.

References

1. Rahhab Z, El Faquir N, Tchetché D, Delgado V, Kodali S, Mara Vollema E, et al. Expanding the indications for transcatheter aortic valve implantation. *Nat Rev Cardiol.* 2020;17:75-84.
2. Van Belle E, Vincent F, Labreuche J, Auffret V, Debry N, Lefèvre T, et al. Balloon-expandable versus self-expanding transcatheter aortic valve

- replacement: a propensity-matched comparison from the FRANCE-TAVI Registry. *Circulation*. 2020;141:243-59.
3. Blackman DJ, Saraf S, MacCarthy PA, Myat A, Anderson SG, Malkin CJ, et al. Long-term durability of transcatheter aortic valve prostheses. *J Am Coll Cardiol*. 2019;73:537-45.
 4. Rheude T, Pellegrini C, Cassese S, Wiebe J, Wagner S, Trenkwalder T, et al. Predictors of haemodynamic structural valve deterioration following transcatheter aortic valve implantation with latest-generation balloon-expandable valves. *EuroIntervention*. 2020;15:1233-9.
 5. Li F, Wang X, Wang Y, Xu F, Wang X, Li X, et al. Structural valve deterioration after transcatheter aortic valve implantation using J-Valve: a long-term follow-up. *Ann Thorac Cardiovasc Surg*. 2020;26:158-65.
 6. Sellers SL, Turner CT, Sathananthan J, Cartledge TRG, Sin F, Bouchareb R, et al. Transcatheter aortic heart valves: histological analysis providing insight to leaflet thickening and structural valve degeneration. *JACC Cardiovasc Imaging*. 2019;12:135-45.
 7. Choi SY, Jeong HJ, Lim HG, Park SS, Kim SH, Kim YJ. Elimination of alpha-gal xenoreactive epitope: alpha-galactosidase treatment of porcine heart valves. *J Heart Valve Dis*. 2012;21:387-97.
 8. Lim HG, Choi SY, Yoon EJ, Kim SH, Kim YJ. In vivo efficacy of alpha-galactosidase as possible promise for prolonged durability of bioprosthetic heart valve using alpha1,3-galactosyltransferase knockout mouse. *Tissue Eng Part A*. 2013;19:2339-48.
 9. Park CS, Park SS, Choi SY, Yoon SH, Kim WH, Kim YJ. Anti alpha-gal immune response following porcine bioprosthesis implantation in children. *J Heart Valve Dis*. 2010;19:124-30.
 10. Park CS, Oh SS, Kim YE, Choi SY, Lim HG, Ahn H, et al. Anti-alpha-Gal antibody response following xenogeneic heart valve implantation in adults. *J Heart Valve Dis*. 2013;22:222-9.
 11. Lim HG, Kim SH, Choi SY, Kim YJ. Anticalcification effects of decellularization, solvent, and detoxification treatment for genipin and glutaraldehyde fixation of bovine pericardium. *Eur J Cardiothorac Surg*. 2012;41:383-90.
 12. Jeong S, Yoon EJ, Lim HG, Sung SC, Kim YJ. The effect of space fillers in the crosslinking processes of bioprosthesis. *Biores Open Access*. 2013;2:98-106.
 13. Lim HG, Choi SY, Jeong S, Shin JS, Park CG, Kim YJ. In vivo efficacy for novel combined anticalcification treatment of glutaraldehyde-fixed cardiac xenograft using humanized mice. *J Biomater Appl*. 2015;29:929-40.
 14. Mangieri A, Montalto C, Pagnesi M, Lanzillo G, Demir O, Testa L, et al. TAVI and post procedural cardiac conduction abnormalities. *Front Cardiovasc Med*. 2018;5:85.
 15. Ussia GP, Barbanti M, Sarkar K, Aruta P, Scarabelli M, Cammalleri V, et al. Transcatheter aortic bioprosthesis dislocation: technical aspects and midterm follow-up. *EuroIntervention*. 2012;7:1285-92.
 16. Ahn CB, Lee SI, Choi CH, Park CH, Park KY, Lee JW, et al. Feasibility of a 3D printed patient-specific model system to determine hemodynamic energy delivery during extracorporeal circulation. *ASAIO J*. 2018;64:309-17.
 17. Lim HG, Kim GB, Jeong S, Kim YJ. Development of a next-generation tissue valve using a glutaraldehyde-fixed porcine aortic valve treated with decellularization, α -galactosidase, space filler, organic solvent and detoxification. *Eur J Cardiothorac Surg*. 2015;48:104-13.
 18. Kim CY, Kim KH, Moon KC, Kim WH, Sung SC, Kim YJ. Comparison of different methods of aortic valve conduit xenograft preservation in an animal experiment model: fresh cryopreservation versus acellularized cryopreservation. *Korean J Thorac Cardiovasc Surg*. 2010;43:11-9.
 19. Park CS, Kim YJ, Lee JR, Lim HG, Chang JE, Jeong S, et al. Anticalcification effect of a combination of decellularization, organic solvents and amino acid detoxification on glutaraldehyde-fixed xenopericardial heart valves in a large-animal long-term circulatory model. *Interact Cardiovasc Thorac Surg*. 2017;25:391-9.
 20. Kim DJ, Kim YJ, Kim WH, Kim SH. Xenograft failure of pulmonary valved conduit cross-linked with glutaraldehyde or not cross-linked in a pig to goat implantation model. *Korean J Thorac Cardiovasc Surg*. 2012;45:287-94.
 21. Lim HG, Kim GB, Jeong S, Kim YJ. Valved conduit with glutaraldehyde-fixed bovine pericardium treated by anticalcification protocol. *Korean J Thorac Cardiovasc Surg*. 2014;47:333-43.
 22. Lim HG, Jeong S, Shin JS, Park CG, Kim YJ. Development of novel combined anticalcification protocols including immunologic modification for prolonged durability of cardiac xenograft: preclinical study using large-animal long-term circulatory models. *ASAIO J*. 2015;61:87-95.
 23. Kim GB, Lim HG, Kim YJ, Choi EY, Kwon BS, Jeong S. Novel self-expandable, stent-based transcatheter pulmonic valve: a preclinical animal study. *Int J Cardiol*. 2014;173:74-9.
 24. Kim GB, Kwon BS, Lim HG. First in human experience of a new self-expandable percutaneous pulmonary valve implantation using knitted nitinol-wire and trileaflet porcine pericardial valve in the native right ventricular outflow tract. *Catheter Cardiovasc Interv*. 2017;89:906-9.
 25. Kim GB, Song MK, Bae EJ, Park EA, Lee W, Lim HG, et al. Successful feasibility human trial of a new self-expandable percutaneous pulmonary valve (Pulsta valve) implantation using knitted nitinol wire backbone and trileaflet α -Gal-free porcine pericardial valve in the native right ventricular outflow tract. *Circ Cardiovasc Interv*. 2018;11:e006494.
 26. Kim MS, Lim HG, Kim YJ. Calcification of decellularized and alpha-galactosidase-treated bovine pericardial tissue in an alpha-Gal knock-out mouse implantation model: comparison with primate pericardial tissue. *Eur J Cardiothorac Surg*. 2016;49:894-900.
 27. Jeong WS, Kim YJ, Lim HG, Jung S, Lee JR. The immune responses and calcification of bioprostheses in the α 1,3-galactosyltransferase knockout mouse. *J Heart Valve Dis*. 2016;25:253-61.
 28. Jang W, Kim YJ, Choi K, Lim HG, Kim WH, Lee JR. Mid-term results of bioprosthetic pulmonary valve replacement in pulmonary regurgitation after tetralogy of Fallot repair. *Eur J Cardiothorac Surg*. 2012;42:e1-8.
 29. Abbas JR, Hoschitzky JA. Which is the best tissue valve used in the pulmonary position, late after previous repair of tetralogy of Fallot? *Interact Cardiovasc Thorac Surg*. 2013;17:854-60.
 30. Giannopoulos AA, Steigner ML, George E, Barile M, Hunsaker AR, Rybicki FJ, et al. Cardiothoracic applications of 3-dimensional printing. *J Thorac Imaging*. 2016;31:253-72.

Key Words: xenograft, heart valve, bioprosthesis, bioengineering, biomaterials, calcification